Elimination of Mismatched Imbalance Vibration of Active Magnetic Bearing System Using Full Order Sliding Mode Controller

Husain A.R.[1], Ahmad M.N.[1] and Mohd Yatim A.H.[1]

[1]*Faculty of Electrical Engineering,*
Universiti Teknologi Malaysia,
81310, Skudai, Johor Bahru, Malaysia
Tel: +60-7-5535894, Fax: +60-7-5544272, E-mail: rashid@fke.utm.my

Abstract

This paper deals with the method to eliminate the vibration inherited in Active Magnetic Bearing(AMB) System due to mass imbalance of the rotor. The imbalance generates variable frequencies of sinusoidal disturbance forces that causes vibration in the system. The mathematical model of the AMB system derived is represented in state variable form and it is also shown that the system suffers the mismatched condition due to this disturbance. The method proposed to overcome the vibration effect is based on full order sliding mode control. In the design process, firstly, a sliding surface is designed that ensures the system is robust to uncertainties once it slides on the surface. Then, a controller that guarantees the system reaches and maintain on the sliding surface is proposed in which Lyapunov stability condition is satisfied. Several simulation result are obtained to evaluate the proposed method. The results show that the proposed controller is able to eliminate the vibration and the robust stability is also achieved.

Keywords:

Sliding Mode Control, Active Magnetic Bearing, Mismatched Rotor Imbalances, Vibration.

1. Introduction

An active magnetic bearing (AMB) system is a collection of electromagnets used to suspend and object and stabilization of the system is performed by feedback control. The system is composed of a floating mechanical rotor and electromagnetic coils that provide the controlled dynamic force. Due to this non-contact operation, AMB system has many promising advantages for high-speed and clean-environment applications. Moreover, adjustable stiffness and damping characteristics also make the system suitable for elimination of system vibration. Although the system is complex and considered an advance topic in term of its structural and control design, the advantages it offers outweigh the design complexity. A few of the AMB applications that receive huge attentions from many research groups around the globe are the flywheel energy, turbo molecular pump, Left Ventrical Assist Device (LVAD) and artificial heart [1].

Other than the gyroscopic effect, the vibration due to mass imbalance of the rotor mass has caused instability of the AMB system and this has imposed great challenge to eliminate the effect. This is due to the fact that the magnitude and frequency of sinusoidal disturbance depends on the rotating speed of the rotor. Also, from the model of AMB system, it can been seen that the vibration term is mismatched with the control input. Many methods have been proposed to overcome the effect such as Q-parameterization [4] [5] and notch filter design [6]. However, the methods are designed at a few rotational speed. In this work, full order sliding mode control (FOSMC) technique will be used to eliminate the vibration effect by performing imbalance compensation where the input voltage will be generated in such a way that the rotor is rotating along its axis of geometry. The method is used due to its robustness towards system uncertainties and parameter variation.

This paper will be organized as follows: In section 2, the derivation of the mathematical modeling of cylindrical AMB system will be covered. In section 3, the synthesis of the FOSMC to remove the mismatched imbalance vibration will be shown. Then, the simulation and the result is discussed in section 4. Finally, the work shown this paper is summarized in the conclusion and a few of future works are outlined.

2. Mathematical Model of Active Magnetic Bearing System

The cross section view of the cylindrical AMB used for the derivation of the mathematical model is shown in Figure 1 below. Four of the voltage supplies, e_{l1}, e_{l2}, e_{l3} and e_{l4} are the top and bottom coils for both left and right that control the vertical motion of the rotor while the voltage supplies for the horizontal motions are e_{l3}, e_{l4}, e_{r3} and e_{r4}. (not shown in Figure 1).

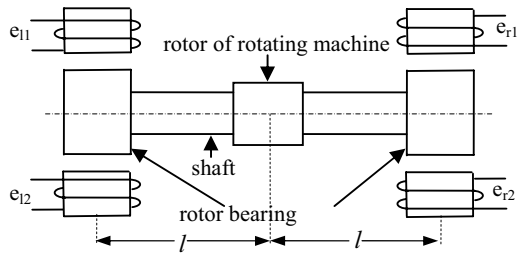

Fig. 1: Cross section view of cylindrical magnetic bearing from *z*-plane

2.1 Equation of motions

Assuming the rotor is rigid floating body, the fundamental equation of motions for the rotor for four degree of freedom are [2][3]

$$\begin{aligned}
\ddot{y}_o &= \frac{1}{m}[\alpha y_o + (f_{l3} \quad f_{l4} + f_{r3} \quad f_{r4}) + f_{dy}] \\
\ddot{z}_o &= \frac{1}{m}[\alpha z_o + (f_{l2} \quad f_{l1} + f_{r2} \quad f_{r1}) + f_{dz} + mg] \\
\ddot{\theta} &= \frac{pJ_x}{J_y}\dot{\psi} + \frac{l}{J_y}((f_{l1} \quad f_{l2} + f_{r2} \quad f_{r1}) + f_{d\theta}) \\
\ddot{\psi} &= \frac{pJ_x}{J_y}\dot{\theta} + \frac{l}{J_y}((f_{l3} \quad f_{l4} + f_{r4} \quad f_{r3}) + f_{d\psi})
\end{aligned} \tag{1}$$

where

- m mass of the rotor
- J_x moment of inertia around x-axis,
- J_y moment of inertia around y-axis
- α radial eccentricity coefficient,
- β axial eccentricity coefficient.

Notice that the movement in x-axis is not included since for cylindrical magnetic bearing, axial motion is uncoupled to other motions and controlled separately. Also, $f_{l1}, f_{l2}, f_{l3}, f_{l4}, f_{r1}, f_{r2}, f_{r3}, f_{r4}$ are the nonlinear magnetic forces produced by the stator coils and exerted on the rotor while $f_{dy}, f_{dz}, f_{d\psi}, f_{d\theta}$ are the sinusoidal disturbance forces caused by the mass imbalance and given by the following equations [5]:

$$\begin{aligned}
f_{dy} &= m_o \varepsilon p^2 \cos(pt + \kappa) \\
f_{dz} &= m_o \varepsilon p^2 \sin(pt + \kappa) \\
f_{d\theta} &= \frac{(J_y \quad J_x)}{l} \tau p^2 \cos(pt + \lambda) \\
f_{d\psi} &= \frac{(J_y \quad J_x)}{l} \tau p^2 \sin(pt + \lambda)
\end{aligned} \tag{2}$$

where

- m_o mass of unbalance
- r radial distance the unbalance mass from rotor center
- ε, τ static and dynamic imbalance
- κ, λ initial values

2.2 Electromagnetic Equations

There are two ways to represent the electromagnetic dynamics which are current based or flux based. Each representation has its advantages [7] and for this work, current-to-force relation is used as shown by equation (3) below in which i_j is the coil current and g_j is the total gap length.

$$f_j = k\left(\frac{i_j}{g_j}\right)^2, \quad j = l1, l2, l3, l4, r1, r2, r3, r4. \tag{3}$$

and k is a constant.

The coil voltage, e_j, which is the input to the system can be expressed in term of i_j, coil inductance L and coil resistance, R. The equation that represents this relation is as follows:

$$e_j = L\frac{di_j}{dt} + Ri_j, \quad j = l1, l2, l3, l4, r1, r2, r3, r4. \tag{4}$$

2.3 Linearization

After integrating equations (1), (2), (3) and (4) above to form a complete cylindrical AMB system, 16 nonlinear equation are formed with 16 states. In order to synthesize the controller that can eliminate the vibration effect, the system is treated to operate around its nominal value with some deviations from this nominal operating conditions. Let F_{oj}, I_{oj}, G_{oj} and E_{oj} be the nominal values of the force, coil current, gap length and electromagnet voltage supplies of the *jth* electromagnet respectively. The deviation value of these quantities are f_j', i_j', g_j' and e_j'. For the deviation value of the force, the partial derivatives of equation (3) is calculated as follows:

$$\frac{\partial f}{\partial g} = k\,i^2\left(\frac{2g}{g^4}\right) = \frac{2ki^2}{g^3} \tag{5i}$$

$$\frac{\partial f}{\partial i} = \frac{2ki}{g^2} \tag{5ii}$$

The quantities derived above is the linearization constants and assumed to be the same for all the electromagnet coils. Thus the quantities can be named as follows:

$$d_j = \frac{2kI_o^2}{G_o^3}, \; c_j = \frac{2kI_o}{G_o^2} \tag{5iii}$$

Then, the following equations can be written for the systems,

$$f_j = F_{oj} + f_j', \; i_j = I_{oj} + i_j', \; g_j = G_{oj} + g_j', \; e_j = E_{oj} + e_j' \tag{6}$$

where

$$f_j' = c_j i_j' + d_j g_j', \quad e_j' = L\frac{di_j'}{dt} + R\, i_j'. \tag{7}$$

For cylindrical horizontal magnetic bearing,

$$\begin{aligned} &d_{l1} = d_{r1},\ d_{l2} = d_{r2},\ d_{l3} = d_{l4} = d_{r3} = d_{r3},\\ &c_{l1} = c_{r1},\ c_{l2} = c_{r2},\ c_{l3} = c_{l4} = c_{r3} = c_{r3}. \end{aligned} \tag{8}$$

Also, the system is controlled in such a way that,

$$e_{l1}' = -\,e_{l2}',\ e_{r1}' = -\,e_{r2}',\ e_{l3}' = -\,e_{r3}',\ e_{l4}' = -e_{r4}', \tag{9}$$

so that the the currents in the coils and force terms will be as follows:

$$i_{l1}' = -\,i_{l2}',\ i_{r1}' = -\,i_{r2}',\ i_{l3}' = -\,i_{r3}',\ i_{l4}' = -i_{r4}', \tag{10}$$

$$\begin{aligned} f_{l1}' - f_{l2}' &= (c_{l1}+c_{l2})i_{l1}' + (d_{l1}+d_{l2})g_{l1}'\\ f_{r1}' - f_{r2}' &= (c_{r1}+c_{r2})i_{r1}' + (d_{r1}+d_{r2})g_{r1}'\\ f_{l3}' - f_{l4}' &= 2c_{l3}\, i_{l3}' + 2d_{l3}g_{l3}'\\ f_{r3}' - f_{r4}' &= 2c_{r3}\, i_{r3}' + 2d_{r3}g_{r3}' \end{aligned} \tag{11}$$

By using gap deviation expression found in [2] and treating $i_y = i_{l3}' + i_{r3}'$, $i_z = i_{l1}' + i_{r1}'$, $i_\theta = i_{l1}' - i_{r2}'$, $i_\psi = i_{l3}' - i_{r3}'$, the new states equation of the AMB system is shown below.

$$\begin{aligned} \ddot{y}_o &= \frac{1}{m}[(\alpha \quad 4d_{l3})y_s + 2c_{l3}i_y + f_{dy}]\\ \ddot{z}_o &= \frac{1}{m}[(\alpha \quad 2d_{l12})z_s \quad c_{l12}i_z + f_{dz}]\\ \ddot{\theta} &= \frac{pJ_x}{J_y}\dot{\psi} + \frac{1}{J_y}(d_{l12}(\quad 2l\theta) + c_{l12}i_\theta + f_{d\theta})\\ \ddot{\psi} &= \frac{pJ_x}{J_y}\dot{\theta} + \frac{1}{J_y}(2d_{l3}(\quad 2l\psi) + 2c_{l3}i_\psi + f_{d\psi}) \end{aligned} \tag{12}$$

Also, from (9) and (10) the following new controlled input voltages can be established:

$$\begin{aligned} e_y &= e_{l3}' + e_{r3}' = L\frac{di_y}{dt} + R\, i_y,\\ e_z &= e_{l1}' + e_{r1}' = L\frac{di_z}{dt} + R\, i_z,\\ e_\theta &= e_{l1}' - e_{r1}' = L\frac{di_\theta}{dt} + R\, i_\theta,\\ e_\psi &= e_{l3}' - e_{r3}' = L\frac{di_\psi}{dt} + R\, i_\psi. \end{aligned} \tag{13}$$

2.4 AMB model in state-space representation

From the equations derived in previous subsection, the system equation now can be converted into state variable form as follows,

$$\begin{bmatrix} \dot{\mathbf{X}}_1\\ \dot{\mathbf{X}}_2\\ \dot{\mathbf{X}}_3\\ \dot{\mathbf{X}}_4 \end{bmatrix} = \begin{bmatrix} \mathbf{A}_y & 0 & 0 & 0\\ 0 & \mathbf{A}_z & 0 & 0\\ 0 & 0 & \mathbf{A}_\theta & \mathbf{A}_{\theta\psi}\\ 0 & 0 & \mathbf{A}_{\psi\theta} & \mathbf{A}_\psi \end{bmatrix} \begin{bmatrix} \mathbf{X}_1\\ \mathbf{X}_2\\ \mathbf{X}_3\\ \mathbf{X}_4 \end{bmatrix} + \begin{bmatrix} b_y & 0 & 0 & 0\\ 0 & b_z & 0 & 0\\ 0 & 0 & b_\theta & 0\\ 0 & 0 & 0 & b_\psi \end{bmatrix} \mathbf{U}(t) + \begin{bmatrix} d_y & 0 & 0 & 0\\ 0 & d_z & 0 & 0\\ 0 & 0 & d_\theta & 0\\ 0 & 0 & 0 & d_\psi \end{bmatrix} \mathbf{d}(t) \tag{14}$$

where

$$\mathbf{X}_1 = \begin{bmatrix} y & \dot{y} & i_y \end{bmatrix}^T,\ \mathbf{X}_2 = \begin{bmatrix} z & \dot{z} & i_z \end{bmatrix}^T,$$
$$\mathbf{X}_3 = \begin{bmatrix} \theta & \dot{\theta} & i_\theta \end{bmatrix}^T,\ \mathbf{X}_4 = \begin{bmatrix} \psi & \dot{\psi} & i_\psi \end{bmatrix}^T.$$

The components for the matrices are given as follows:

$$\mathbf{A}_y = \begin{bmatrix} 0 & 1 & 0\\ \dfrac{\alpha \quad 4d_{l3}}{m} & 0 & \dfrac{2c_{l3}}{m}\\ 0 & 0 & R/L \end{bmatrix},$$

$$\mathbf{A}_z = \begin{bmatrix} 0 & 1 & 0\\ \dfrac{\alpha \quad 2d_{l12}}{m} & 0 & \dfrac{c_{l12}}{m}\\ 0 & 0 & R/L \end{bmatrix},$$

$$\mathbf{A}_\theta = \begin{bmatrix} 0 & 1 & 0\\ \dfrac{2d_{l12}}{m_1} & 0 & \dfrac{c_{l12}}{lm_1}\\ 0 & 0 & R/L \end{bmatrix},$$

$$\mathbf{A}_\psi = \begin{bmatrix} 0 & 1 & 0\\ \dfrac{4d_{l3}}{m_1} & 0 & \dfrac{2c_{l3}}{lm_1}\\ 0 & 0 & R/L \end{bmatrix},$$

$\mathbf{A}_{\theta\psi} = diag\,(0, \frac{pJ_x}{J_y}, 0)$, $\mathbf{A}_{\psi\theta} = diag\,(0, \frac{pJ_x}{J_y}, 0)$,

$\mathbf{U}(t) = \begin{bmatrix} e_y & e_z & e_\theta & e_\psi \end{bmatrix}^T$, $b_y = b_z = b_\theta = b_\psi = diag\,(0,0,1/L)$,

$d_y = d_z = diag\,(0,\ 1/m,\ 0)$, $d_\theta = d_\psi = diag\,(0,\ 1/m_1,\ 0)$,

$m_1 = J_y / l^2$ and $\mathbf{d}(t) = [f_{dy}\ f_{dz}\ f_{d\theta}\ f_{d\psi}]^T$.

From this state equation, it can be seen that the system can be decoupled into 3 subsystems with 2 SISO systems that govern the y and z motions and 1 MIMO system that describe both θ and ψ motions. The controller derived in the next section will be based on these 3 subsystem in which

the vibration components in each subsystem will be eliminated.

3. Full Order Sliding Mode Controller (FOSMC) Design

The state equation (14) above can be written as

$$\dot{X}(t) = AX(t) + BU(t) + f(t) \qquad (15)$$

where $f(t)$ is the vibration term with the mismatched condition i.e. *rank* $[B,f(t)] \neq$ *rank* $[B]$ in which this term is not in phase with the system input. Thus, the proposed controller should be robust enough to overcome the mismatched vibration term to ensure stability of the system performance can be achieved.

Let the PI Sliding Surface be defined as [8]:

$$s(t) = C\mathbf{X}(t) - \int_0^t [CA\text{-}CBK]\,\mathbf{X}(\tau)d(\tau) \qquad (16)$$

where $C \in$ ^{mxn} and $K \in$ ^{mxn} are constant matrices. The matrix C is chosen such that $CB \in$ ^{mxm} is non-singular while the matrix K satisfies $\lambda_{max}(A + BK) < 0$. This condition will guarantee that all desired poles are located in the left-hand plane to ensure system stability. It is well known that if the system is able to enter the sliding mode, $s(t) = 0$. Then, the equivalent control, U_{eq} can be determined by letting $\dot{s}(t) = 0$ and substituting the equation into (15) producing

$$U_{eq} = KX(t) - (CB)^{-1}Cf(t) \qquad (17)$$

Substituting (17) into system equation (15) gives the equivalent dynamic equation of the system when sliding on the surface as:

$$\dot{X}(t) = (A + BK)X(t) + \{I_n \quad B(CB)^{-1}C\}f(t) \qquad (18)$$

Notice that the system will be asymptotically stable if vibration term is matched eliminating the second term in (18). Due to this mismatched condition, the following theorem is introduced.

Theorem 1: If $\|\tilde{F}(t)\| \quad \beta_1 = \|I_n \quad B(CB)^{-1}C\|\beta$, the uncertain system equation (18) is boundedly stable when sliding surface.

Proof: See [9].

For the controller design that can drive the system states to slide on sliding surface and ensure system remains boundedly stable thereafter , the controller of the following form is proposed:

$$U = U_{eq} + U_{nl} \qquad (19)$$

where the total control effort U is composed of equivalent control, U_{eq} derived in (17) and nonlinear control, U_{nl}. The equivalent control is stabilizing the system on sliding surface and the nonlinear control is the nonlinear feedback control that supress the disturbance and forcing the system to switch on the designed surface. Thus, the following control law is proposed:

$$U(t) = KX(t) - (CB)^{-1}Cf(t) - (CB)^{-1}\rho sgn(s(t)) \qquad (20)$$

The proposed controller guarantees the hitting condition is met and the proof can be found in [9][10]. Notice that the signum function, $sgn(t)$, is a switching function that cause chattering. However, in this work the main objective is vibration elimination and chattering elimination is not the main focus. Thus the function is maintained in the controller.

4. Simulations and results

The simulation of the AMB system and proposed controller is performed by using the following parameters shown in Table 1 [3][4].

Table 1: Parameters for Active Magnetic Bearing

Parameter	Symbol	Value
Mass of rotor (*kg*)	m	13.9
Moment of inertia about X ($kg.m^2$)	J_x	0.0134
Moment of inertia about Y ($kg.m^2$)	J_y	0.232
Half the longitudinal length (*m*)	l	0.13
Steady state gap length (*mm*)	G_o	0.55
Rotational speed(*rad/sec*)	p	0- π50
Coil resistance (*ohm*)	R	10.7
Coil inductance (*H*)	L	0.285
Radial eccentricity (*N/m*)	α	0
Steady state attractive force for left and right (*N*)	$F_{l1,r1}$ $F_{l1\text{-}l4,r2\text{-}r4}$	90.9 22
Steady state current for left and right coils (*A*)	$I_{l1,r1}$ $I_{l1\text{-}l4,r2\text{-}r4}$	0.63 0.31

For the selection of the controller gain K, pole placement method is used in which the poles is selected to reside on the left-hand plane to ensure system stability. Thus for this case, two set of 3 poles and a set of 6 poles are selected for the above 2 SISO and 1 MIMO system. The calculated K values for each subsystems with their respective poles selections are as follows:

1st subsystem: $K_1 = 10^7[1.2016 \;\; 0.0001 \;\; 0.0008]$, for poles $\lambda_1 = \{-7500, -10555, -11100\}$,

2nd subsystem: $K_1 = 10^7[-1.0804 \;\; -0.0001 \;\; 0.0006]$, for poles $\lambda_2 = \{-5900, -6555, -7100\}$,

3rd subsystem:

$$K_3 = 10^6 \begin{matrix} 2.1721 & 0.0001 & 0.0085 & 0.1102 & 0.0 & 0.0006 \\ 0.4246 & 0.0 & 0.0016 & 1.3757 & 0.0001 & 0.0086 \end{matrix}$$

for poles

λ_3 = { -6500 -6900 -8100 -9900 -11900 -16700}.

The same gain K for all the subsystems are used for feedback control (pole placement) used to compare the performance of the designed controller to overcome the vibration. Next for the selection of the controller matrix C, the following values are chosen:

1st subsystem: C_1 = [3.8493 0.0002 0.0019],
2nd subsystem: C_2 = [9.8522 0.0002 -0.0045],
3rd subsystem:

$$C_3 = 10^4 \begin{matrix} 3.7370 & 0.0001 & 0.0115 & 0.3608 & 0.0 & 0.002 \\ 4.2208 & 0.0001 & 0.0130 & 0.4075 & 0.0 & 0.0023 \end{matrix}$$

In selecting the values for matrix C, a simple optimization algorithm is used in which a set of simultaneous equations are solved and these values are used to access the system performance. The process is repeated until the performance of the system is satisfied.

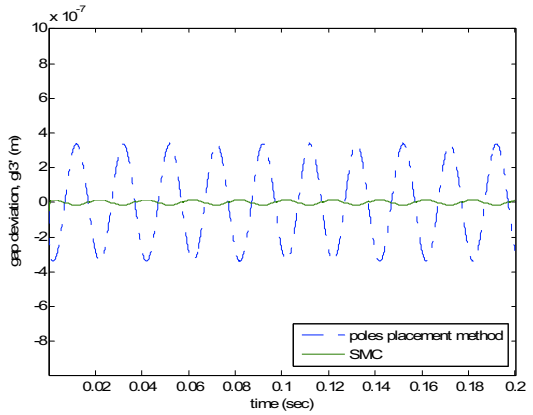

Fig. 2: Comparison of gap deviation for g_{l3}' between robust controller and pole place method.

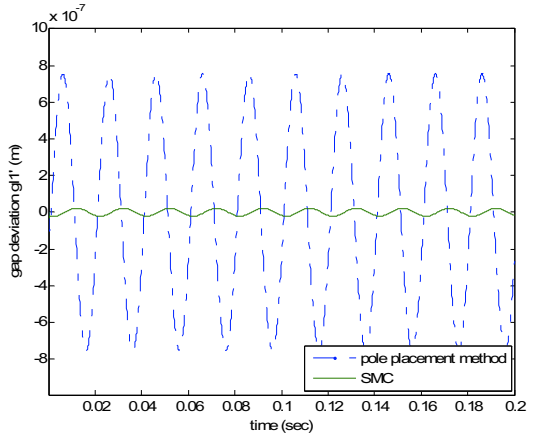

Fig. 3: Comparison of gap deviation for g_{l1}' between robust controller and pole place method.

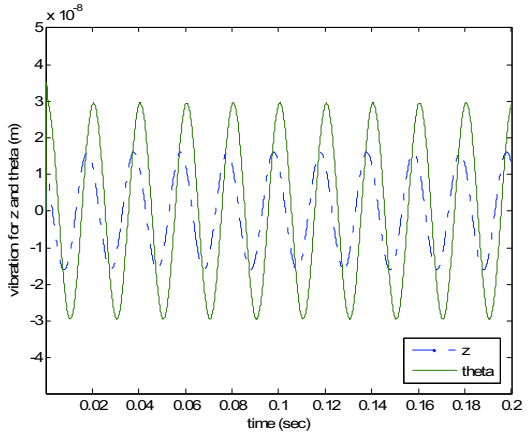

Fig. 4: The displacement for z-axis and θ motion

Vibration magnitude below 0.5 micron is considered an acceptable performance for most AMB system. Figure 2 above illustrates the the gap deviation, g_{l3}', which is the magnitude of vibration on the left horizontal of the system. The amplitude of the vibration is only about 0.016 micron which is very low and considered zero relative to the total gap. Comparing to pole placement method, the amplitude of vibration is 0.35 micron which is close to upper side of acceptable range, the proposed controller is able to suppress the vibration about 22 times further. Figure 3 shows the gap deviation, g_{l1}', on the left vertical of the system. The same performance can be noticed in which the magnitude of vibration under the robust controller is extremely low and equivalent to zero. Figure 4 then shows the component of vibration in the z-axis motion and θ motion. These two components contribute to the vibration of rotor in vertical movement. The figure shows the magnitude in both motions under the proposed controller. In this case the vibration in z-axis motion is a little larger than the vibration in θ motion which suggest that the C parameter for the SISO subsystem of z- motion can further be tuned. Figure 5 illustrates the sinusoidal magnetic force produced by the coil in order to compensate the vibration term present in the system.

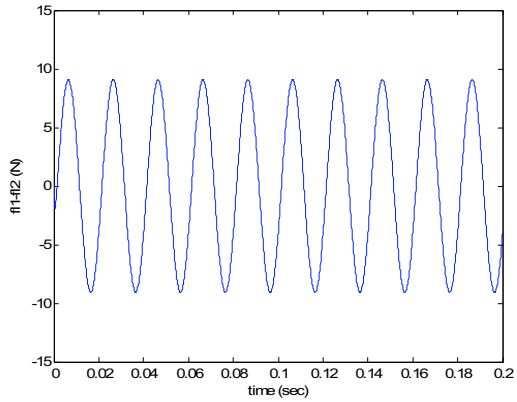

Fig. 5: Magnetic force acting on the magnetic bearing.

5. Conclusion

This paper concerns with design of full order sliding mode control method that can eliminate the rotor vibration due to mass imbalance. After deriving the dynamic model of the system and presented in state-space representation, it is shown that this vibration term also suffers mismatched condition in which it is not in phase with the input voltage. Based on proportional integral sliding mode design, the robust controller proposed is able to suppress the vibration and solve the mismatched problem. Simulation results show that the vibration is kept to a very minimum range and fulfil the design requirement. However, tuning of the controller parameter is quite time consuming and a more intelligent method will improve the overall design. This will be the next step of this work.

REFERENCES

[1] Lee J.H.; Allaire P. E.; Tao G.; Decker J.; and Zhang X. 2003. Experimental Study of Sliding Mode Control for a Benchmark Magnetic Bearing System and Artificial Heart Pump Suspension. *IEEE Trans. on Contr. Sys. Tech*., vol. 11, no. 1.

[2] Matsumura F.; and Yoshimoto T. 1986. System Modeling and Control Design of a Horizontal-shaft Magnetic Bearing System. *IEEE Trans. on Magnetics*., vol. MAG-22, no. 3.

[3] Matsumura F.; Fujita M.: and Okawa K. 1990. Modeling And Control of Magnetic Bearing Systems Achieving A Rotation Around the Axis of Inertia. In proceedings of the 2nd International Symposium on Magnetic Bearings, 273-280. Tokyo, Japan.

[4] Mohamed A. M.; Matsumura F.; Namerikawa T.; and Lee J. H. 1997. Q-Parameterization Control of Vibrations In A Variable Speed Magnetic Bearing. In *Proceedings Of IEEE International Conference on Control Applications*, 540-545. Hartford, CT.

[5] Mohamed A. M.; Hassan I. M.; Hashem A. M. K. 1999. Elimination of Imbalance Vibrations in Magnetic bearing System Using Discrete-Time Gain-Scheduled Q-Parameterization Controllers. In *Proceedings Of IEEE Conf. Int, Conf. on Contr Application*, 737-741. Kohala Coast-Island of Hawai'i, Hawai'i.

[6] Herzog R. ; Buhler P. ; Gahler C. ; and Larsonneur R. 1996. Unbalance Compensation Using Generalized Notch Filters in the Multivariable Feedback of Magnetic Bearings. *IEEE Transactions on Control Systems Technology*. Vol. 4, No. 5.

[7] Mohamed A. M.; and Emad F. P. 1993. Comparison Between Current and Flux Control in Magnetic Bearing Systems. In *Proceedings. of the American Control. Conference.*

[8] Yan J.J.; Tsai J.S.-H; and Kung F. –C. 1997. Robust Decentralized Stabilization of Large-Scale Delay Systems Via Sliding Mode Control. *ASME Journal of Dynamic Systems, Measurement and Control*. 307-312.

[9] Sam Y. M.; and Osman J. H. S. 2003. Active Suspension Control: Performance Comparison using Proportional Integral Sliding Mode and Linear Quadratic Regulator Methods. In *Proceedings in Control Application Conference*. 274-278.

[10] Cristi R. ; Papoulias F. A. ; and Healey A. J. 1990. Adaptive Sliding Mode Control of Autonomous Underwater Vehicles in the Dive Plane. *IEEE Journal of Oceanic Engineering*. Vol 15, No. 3.